Using Imaging Spectroscopy to Study Ecosystem Processes and Properties

SUSAN L. USTIN, DAR A. ROBERTS, JOHN A. GAMON, GREGORY P. ASNER, AND ROBERT O. GREEN

Remote sensing data provide essential input for today's climate and ecosystem models. It is generally agreed that many model processes are not accurately depicted by current remotely sensed indices of vegetation and that new observational capabilities are needed at different spatial and spectral scales to reduce uncertainty. Recent advances in materials and optics have allowed the development of smaller, more stable, accurately calibrated imaging spectrometers that can quantify biophysical properties on the basis of the spectral absorbing and scattering characteristics of the land surface. Airborne and spaceborne imaging spectrometers, which measure large numbers (hundreds) of narrow spectral bands, are becoming more widely available from government and commercial sources; thus, it is increasingly feasible to use data from imaging spectroscopy for environmental research. In contrast to multispectral sensors, imaging spectroscopy produces quantitative estimates of biophysical absorptions, which can be used to improve scientific understanding of ecosystem functioning and properties. We present the recent advances in imaging spectroscopy and new capabilities for using it to quantify a range of ecological variables.

Keywords: remote sensing, landscape ecology, imaging spectroscopy, hyperspectral imaging, spectral analysis

The consequences of land use, disturbance, and climate change in the world's ecosystems have created increased demand for remote sensing data at all scales. A wide range of information is needed to predict the consequences of climate change and to monitor carbon, water, and nutrient cycles, from land cover, land-use history, and estimates of standing biomass to succession, biodiversity, and sustainability. Traditional field-based sampling methods are prohibitively expensive and time-consuming at large spatial scales, and such methods are inadequate for today's needs. Satellite observations provide the only practical means to obtain a synoptic view of Earth's ecosystems, including their spatial distribution, extent, and temporal dynamics (Cohen and Goward 2004).

Accurate maps of the spatial distribution, percentage cover, and variability of global ecosystems are essential to improve ecosystem process models (Running et al. 2004, Turner et al. 2004). Current vegetation maps contain significant classification errors, and there is little understanding of how to scale mixed land cover, variable stand age, and density classes from local estimates. Normalized difference vegetation index (NDVI) data are used for estimating carbon fluxes, stores, and turnover rates, as well as other land-cover characteristics affecting the carbon budget. However, ecosystem and biogeochemical models could significantly benefit from independently derived information about terrestrial biomes. Several new types of data that could improve model results, including quantitative estimates of canopy and soil biochemistry, canopy structural information, and improved land-cover classifications, can be produced by imaging spectrometers.

A wide range of new instrument capabilities are available or planned, based on airborne and satellite platforms that measure all parts of the electromagnetic spectrum, from ultraviolet to radar (Treuhaft et al. 2004). Imaging spectrometers are instruments that measure a detailed spectrum of reflected solar energy for each pixel. Spectroscopy data have already significantly improved theoretical understanding of the interactions of electromagnetic radiation with matter and are changing the way remotely sensed data are analyzed

Susan L. Ustin (e-mail: slustin@ucdavis.edu) is a professor of environmental and resource sciences in the Department of Land, Air, and Water Resources, University of California, Davis, CA 95616. Dar A. Roberts is a professor in the Department of Geography, University of California, Santa Barbara, CA 93106. John A. Gamon is an associate professor in the Department of Biology and Microbiology, California State University, Los Angeles, CA 90032. Gregory P. Asner is a faculty scientist in the Department of Global Ecology, Carnegie Institution of Washington, Stanford, CA 94305. Robert O. Green is an AVIRIS (Airborne Visible/Infrared Imaging Spectrometer) experiment scientist in the Observational Instruments Division, Jet Propulsion Laboratory, California Institute of Technology, Pasadena, CA 91109.

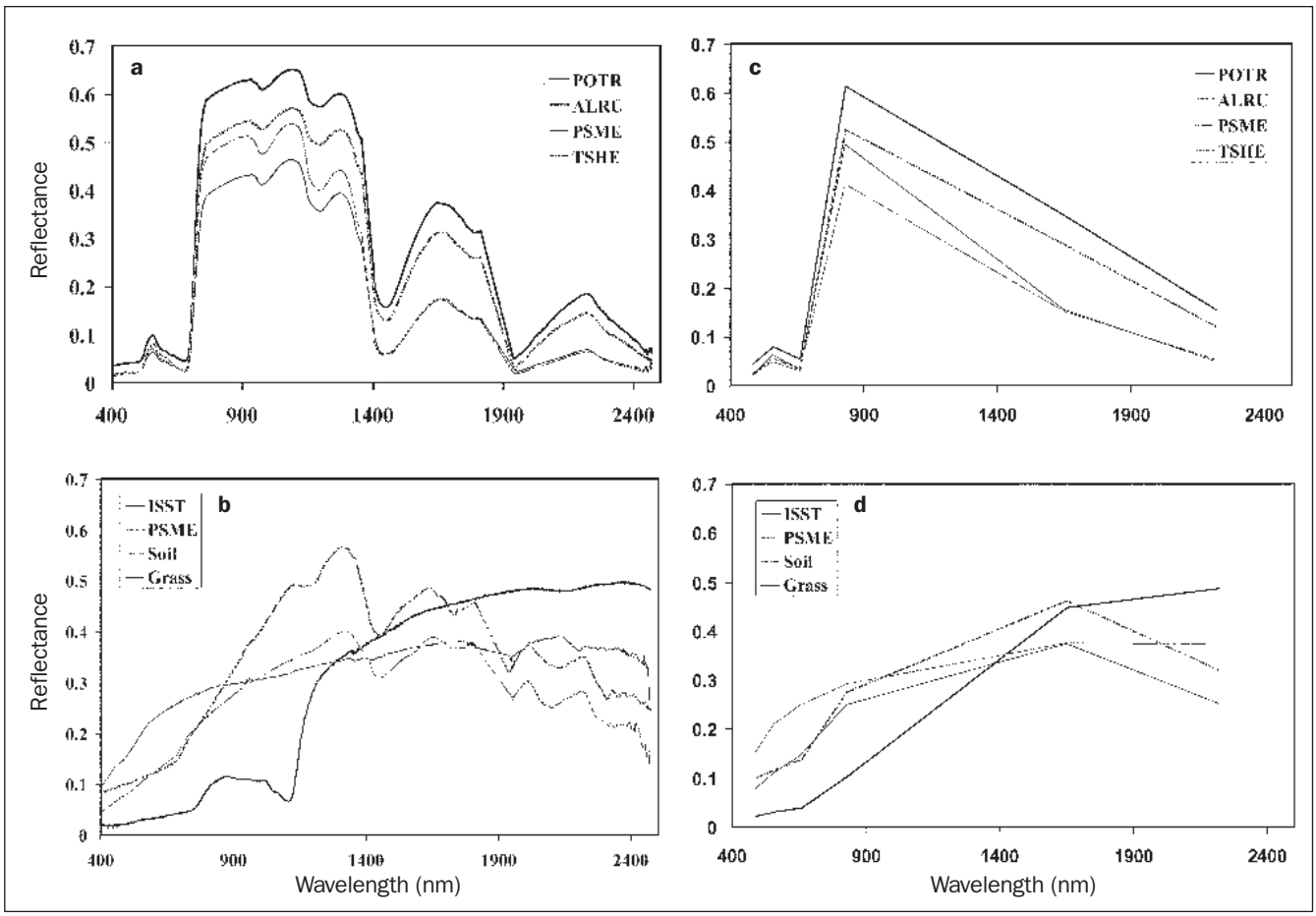

Figure 1. (a) Detailed mean spectra from four live tree species with green foliage:* Populus trichocarpa *(POTR, black cottonwood),* Alnus rubra *(ALRU, red alder),* Pseudotsuga menziesii *(PSME, Douglas fir), and* Tsuga heterophylla *(TSHE, western hemlock). (b) Three types of "less-green" plant materials (*Isothecium stoloniferum *[ISST, epiphytic lichen], PSME bark, dry grass) and soil. (c) Landsat six-band spectra of species shown in panel a. (d) Landsat six-band spectra of less-green materials shown in panel b.

by emphasizing biophysical interpretations that are based on quantitative measurements of physical properties.

Imaging spectrometers

Most landscapes are spatially and compositionally complex, which makes one- to six-band multispectral observations inherently underdetermined (Asner 1998). Figure 1 (panels c and d) illustrates the similarity of five vegetation types measured by a multispectral Landsat instrument. When considering a landscape with mixed communities and variable plant densities, it is clear why more spectral information is desirable. Imaging spectrometers (sometimes called "hyperspectral" imagers because of their many narrow spectral bands) measure the reflected solar spectrum from 350 to 2510 nanometers (nm) with 150 to 500 contiguous bands of 5- to 10-nm bandwidths. The full spectra of these vegetation types (figure 1a, 1b) demonstrate the spectral variability among species and the enhanced information content in spectroscopy data relative to multiband data.

Spectroscopy from aircraft and satellites is a new field of research, established in the 1990s, that relies on measuring the interactions between matter and electromagnetic radiation to identify properties and processes at Earth's surface. There are currently more than a dozen operational airborne imaging spectrometers (Wulder 1998), most of which are restricted to measuring the visible and near-infrared regions (400 to 1000 nm). However, a few airborne imagers (e.g., the Airborne Visible/Infrared Imaging Spectrometer [AVIRIS], developed by the National Aeronautics and Space Administration [NASA], and the commercial HyMap, developed by Integrated Spectronics Corporation, Australia) and spaceborne imagers (e.g., Hyperion on the EO-1 satellite) measure the spectrum from 400 to 2500 nm. AVIRIS, HyMap, and Hyperion have 224, 158, and 200 adjacent spectral bands, respectively. A number of other satellite instruments are planned for launch in this decade, including the European Space Agency's SPECTRA (Surface Processes and Ecosystem Changes through Response and Analysis) and a proposed Canadian imaging spectrometer. Although the numbers of

these instruments and their data remain limited, they have demonstrated the power to provide ecological information that is unavailable from other technologies.

The absorbing and scattering properties of natural surfaces are defined by their chemical bonds and by their three-dimensional structure, which determines their reflectance spectra. Analysis of the spectra of these surfaces permits spatial mapping of their biogeochemical features. Narrow spectral bands can measure many individual absorption features of interest to ecologists, such as pigment composition and content (Lichtenthaler et al. 1996, Gitelson and Merzlyak 1997), canopy water content (Peñuelas et al. 1997, Ustin et al. 1998), canopy dry plant litter or wood (Roberts et al. 1993, Asner et al. 1998), and other aspects of foliar chemistry (Curran 1989, Martin and Aber 1997).

The wavelength region of optical observations extends from 400 nm in the visible to 2500 nm in the reflected solar infrared spectrum. The strong absorption of light by photosynthetic pigments in green foliage dominates the visible spectrum (400 nm to 700 nm; figure 1a). The detection of specific photosynthetic pigments, including chlorophyll *a* and *b* xanthophylls (e.g., violaxanthin, zeaxanthin), carotenes, and unique algal pigments (e.g., chlorophylls *c* and *d,* phycobilin), is an active area of research with great promise for future applications.

The near-infrared (700 to 1100 nm) is a region of high reflectance with limited biochemical absorption. Most absorption in this region involves water (at 870 and 1240 nm) and compounds typical of dry leaves; the latter are primarily cellulose, lignin, and other structural carbohydrates that have broad, weak absorptions across the region (figure 1a, 1b). Reflectance is dominated by multiple scattering of photons by the internal structure, air spaces, and air-water interfaces that refract light within leaves. The shortwave-infrared (1100 to 2500 nm) is another region of low reflectance and strong absorption, primarily by water in green leaves (figure 1a). In dry leaves, shortwave-infrared reflectance (figure 1b) is dominated by the presence of carbon compounds such as cellulose and lignin and by other plant biochemicals, including nitrogen, starches, and sugars that have overlapping absorbances in this region. Curran (1989) summarized the wavelength locations of bond vibrations for single (–) and double (=) bonds between carbon, hydrogen, nitrogen, and oxygen atoms (C–H, C–O, C–O–C, C=O, N–H, N=H, O–H, and O=H) that would be characteristic of these compounds. For example, N–H bonds have a first harmonic overtone at 1510 nm and a series of combination bands at 1980, 2060, and 2180 nm (Wessman 1990) and at 2054 and 2168 nm (Davies and Grant 1988). Cellulose has a broad absorption feature at 2104 nm, but starch and hemicellulose also have absorptions in this region, which limits researchers' ability to uniquely identify these compounds (Kokaly 2001). The simultaneous measurement of the full spectrum, however, provides the most powerful basis for identifying biochemical composition.

Calibration of spectra to apparent surface reflectance

The data from imaging spectrometers, like those from multiband imagers, are acquired as digital numbers or electronic counts that depend on the characteristics of the detector and the amount of energy received. These raw data are calibrated to produce a measure of radiance (watts per steradian per square meter [m^2]) by laboratory calibration of the detector response function. Although spectroscopy data can be statistically analyzed using either the digital numbers or the radiance values, the true power of these data is realized only when they are further processed to surface reflectance. This correction, though rarely applied to multispectral data, adjusts for sun and view angle effects and differences in atmospheric conditions. After calibration has produced a measure of surface reflectance, the data can be compared to field or laboratory spectra or to other image data sets for identification and analysis (figure 2). Calibration of data to reflectance permits analysis using searches for specific spectral signatures. Further, by standardizing the data to the incoming solar flux, it allows the detection of small changes in reflectance, often near the instrument noise level, which indicate a change in the abundance of specific materials.

The upper right panel in figure 2 shows the "true" upwelling spectral radiance measured at the top of the atmosphere. The middle panel illustrates raw data at the top of the atmosphere as measured by the sensor. These data must be calibrated to account for instrument performance, producing a simplified radiance spectrum (shown in the lower left panel) that approximates the true radiance. To make full use of the spectral data from an imaging spectrometer, the radiance data are calibrated to yield apparent surface reflectance using a radiative transfer model that accounts for the scattering and absorbing properties of gases in the atmosphere. The lower right panel in figure 2 shows the surface reflectance of the vegetated pixel after calibration, with the resulting spectrum closely matching a plant spectrum as measured in the field (figure 2, upper left panel).

Detection and mapping of canopy and soil biogeochemical properties

The goal of mapping biogeochemical properties in ecological studies is to provide information about ecosystem conditions, and particularly about the locations and types of environmental stresses. Because of the importance of photosynthetic function, most research has focused on the spectral properties of leaves and canopies that provide estimates of chlorophyll, water, dry matter, and nitrogen (Turner et al. 2004). Senescent leaves follow a typical trajectory, with decreases in chlorophyll followed by losses of other pigments and water. Aging and stress increase reflectance over the visible and shortwave-infrared spectrum and decrease it in the near-infrared. The difference in reflectance between the visible and near-infrared regions is the basis of vegetation indices (e.g., NDVI). However, using the full spectrum in a radiative

transfer model (e.g., PROSPECT; Jacquemoud et al. 1995, 1996) produces quantitative estimates of biochemical content.

Photosynthetic pigments

Loss of chlorophyll (chlorosis) increases reflectance across the visible and near-infrared spectrum and shifts the red edge (the long-wavelength edge of the chlorophyll absorption) toward shorter wavelengths (termed the "blue shift"). Rock and colleagues (1988) found a blue shift in spruce and fir sites exposed to atmospheric pollution, which they attributed to a decrease in chlorophyll *b* and total chlorophyll. Measuring the shift in wavelength position requires an instrument with 1- to 5-nm resolution, because the shift is often less than 25 nm.

Spectrometers can be used to detect relative levels of major plant pigment classes, including chlorophylls (green pigments), carotenoids (yellow-orange pigments), and anthocyanins (red-purple pigments). These pigment levels can indicate conditions of stress, assess photosynthetic activity, and map vegetation. Direct measurement of chlorophyll concentration requires controlling for variable leaf area. A number of studies have inverted linked leaf and canopy models to estimate chlorophyll content or separate chlorophyll and leaf area index (LAI) (Weiss and Baret 1999).

Biochemical differences (e.g., pigment or water levels) can be used to map vegetation (figure 3). A variety of methods (e.g., spectral mixture analysis) can be applied to decompose landscapes into areas with different predominating component pigments. These areas can be recombined into images, as in figure 3, in which chlorophylls, carotenoids, and anthocyanins are mapped separately and then composited. Additional dimensions can be provided by including other plant biochemicals (e.g., water). The resulting approach provides a powerful method for classifying vegetation, with different classes occupying different trajectories within the

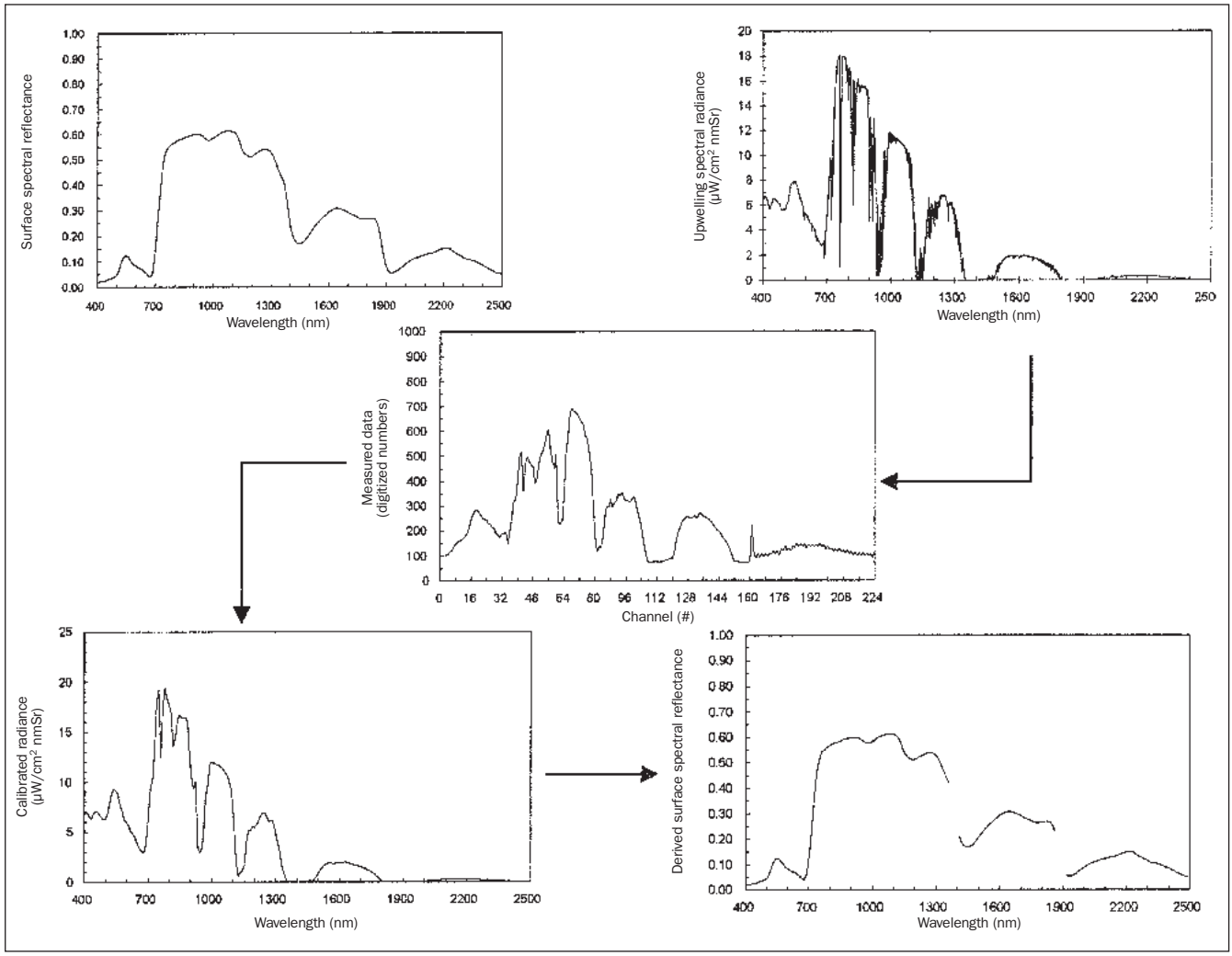

Figure 2. Processing measured spectra to surface reflectance. Upper left: Typical plant canopy spectrum measured in the field. Upper right: Upwelling spectral radiance at the top of the atmosphere. Middle: Digital number count measured by the sensor. Lower left: Calibrated radiance. Lower right: Derived surface reflectance after atmospheric calibration using a radiative transfer model. Missing wavelength segments in derived surface reflectance are areas of atmospheric water vapor absorption where no energy is measured.

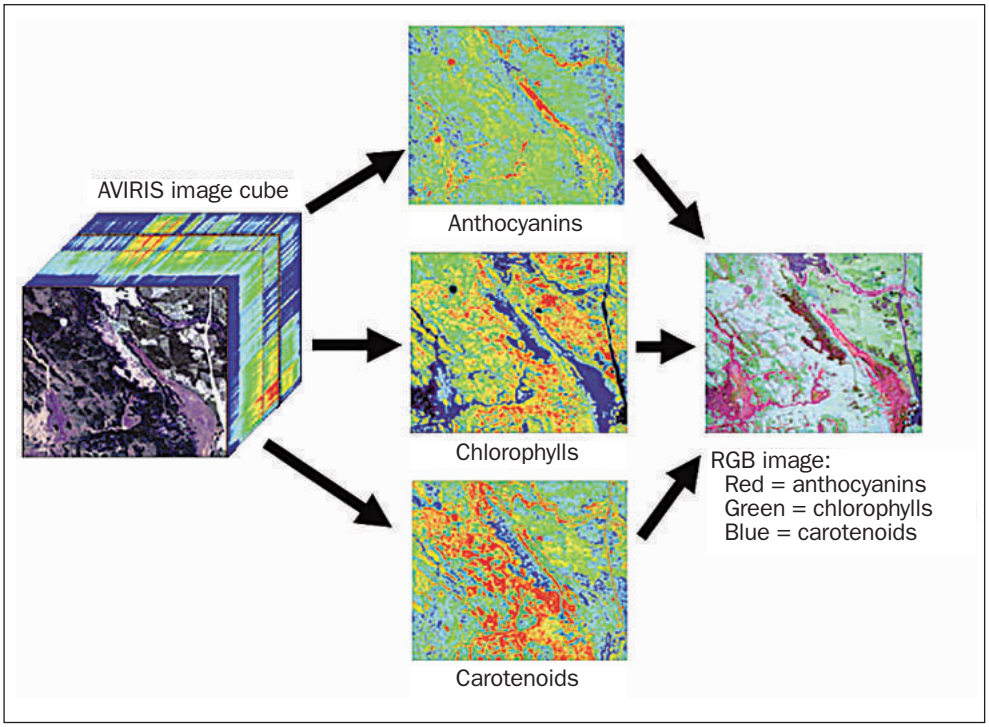

Figure 3. Pigment-based landscape classification for a Canadian boreal forest region using the National Aeronautics and Space Administration's AVIRIS (Airborne Visible/Infrared Imaging Spectrometer). The image cube (left) shows a three-band natural-color image on the face and, in the receding dimension, a color-coded spectrum of the edge pixels in which reflectance values are ordered from lowest to highest: black, blue, green, yellow, orange, and red. The relative concentrations of anthocyanins, chlorophylls, and carotenoids (center) were estimated by a spectral mixture analysis that separated these pigments following the method of Fuentes and colleagues (2001). The composite color image (right) shows a landscape classification based on these pigments. Source: Courtesy of David Fuentes.

resulting multidimensional volume. This biochemical method has been successfully applied to map boreal forests (Fuentes et al. 2001) and chaparral vegetation.

Subtle changes in pigment ratios—anthocyanin and chlorophyll-carotenoid ratios in particular—can reveal plant stress or altered photosynthetic activity. For example, the photochemical reflectance index was originally formulated to indicate diurnal interconversion of xanthophyll cycle pigments that are closely tied to photosynthetic activity (Gamon et al. 1992). Recent work has demonstrated that over seasonal periods, this index measures relative levels of chlorophylls and carotenoids and reveals spatial and temporal patterns of photosynthetic activity for entire ecosystems (e.g., Rahman et al. 2001). Because the component processes affecting these pigment indices are often confounded, interpretations should carefully consider the contributions of both physiological and structural components (Barton and North 2001). Newer approaches involve the inversion of spectra in radiative transfer models and may yield improvements over index approaches, but these approaches remain difficult to apply in practice.

Plant water content

Remotely estimating canopy water content is important for assessing drought and predicting susceptibility to wildfire (Ustin et al. 1998). The primary and secondary effects of water content on leaf reflectance are greatest in spectral bands centered at 1450, 1940, and 2500 nm (Carter 1991); with indirect or secondary effects at 400 nm; in the red edge at 700 nm (Filella and Peñuelas 1994); and with NDVI. Many band ratios have been proposed to estimate water content, including the normalized difference water index (NDWI; Gao 1996) and the plant water index (PWI; Peñuelas et al. 1997). Gao and Goetz (1995) calculated an equivalent water thickness (EWT; i.e., the depth of water across the pixel) by fitting a water spectrum across the feature centered at 980 nm (figure 4a). Zhang and colleagues (1996) and Sanderson and colleagues (1998) used this absorption feature to map canopy water content in salt marshes; Ustin and colleagues (1998) used it to map water content in a semiarid shrubland.

Serrano and colleagues (2000) demonstrated that the PWI and NDWI were affected by canopy structure and viewing geometry, and Zarco-Tejada and Ustin (2001) demonstrated

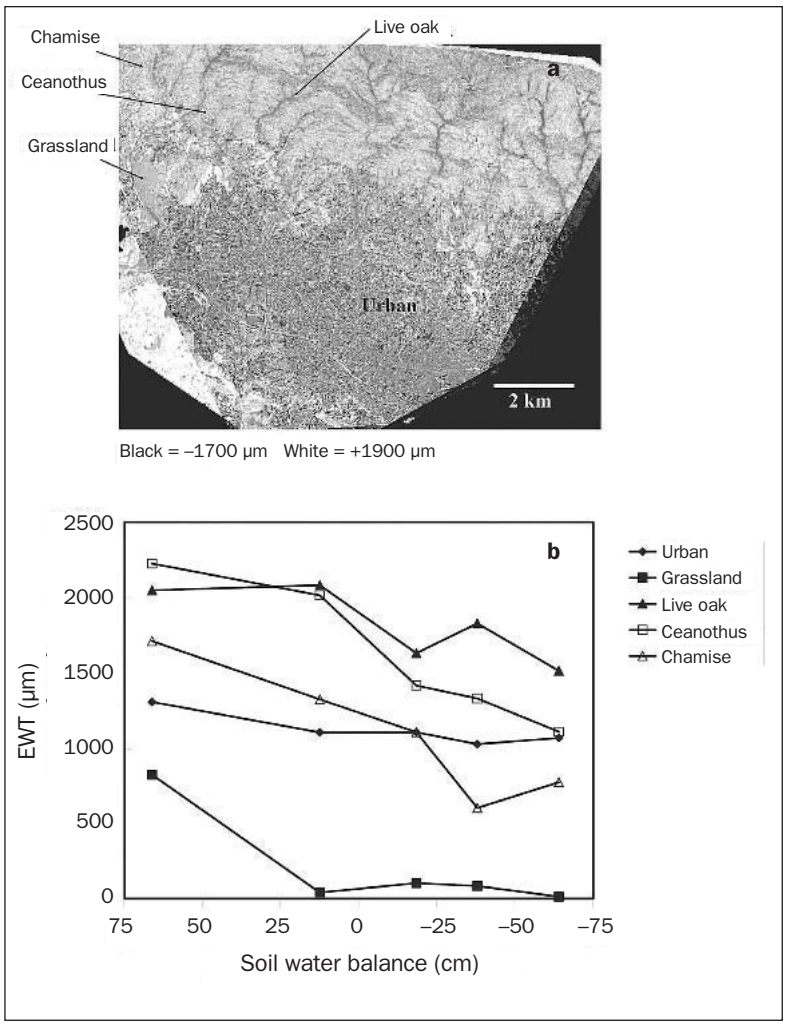

Figure 4. (a) The difference in equivalent water thickness (EWT) between 30 May 1998 and 11 September 1999, derived from AVIRIS (Airborne Visible/Infrared Imaging Spectrometer) data. Light areas had more water in May; dark areas had more water in September. (b) EWT measured by AVIRIS on five dates for five vegetation types compared with field-measured soil water balance.

the dependency of these indexes on leaf structure, dry matter content, and LAI. Accurate quantitative estimates of water content can be derived using the full spectrum analyzed in a radiative transfer model such as PROSPECT (Jacquemoud et al. 1995, 1996) or LEAFMOD (Leaf Experimental Absorptivity Feasibility Model; Ganapol et al. 1998) for broadleaf species, or LIBERTY (Dawson et al. 1998) for needleleaf species.

Figure 4 illustrates seasonal changes in EWT for different vegetation types near Santa Barbara, California, measured by AVIRIS. Figure 4a shows the difference in EWT measured during a wet El Niño spring and late in the summer drought. Grasslands and shrublands have lower EWT in September than in May; both grasslands and shrublands have lower water content than the riparian oaks (primarily live oak, or *Quercus agrifolia*). Urban areas exhibit little seasonal change in EWT and are similar to the riparian oaks in water content. The EWT for five classes of land cover decreases as soil water balance (cumulative difference between precipitation and evapotranspiration) becomes more negative (figure 4b; Dennison and Roberts 2003a). The AVIRIS data are shown for five dates, ranging from an extremely wet to an extremely dry period. The largest changes occurred while soil water balance remained positive: EWT decreased in ceanothus (*Ceanothus* spp.) by 1100 micrometers (µm) per pixel (400 m^2), in chamise (*Adenostoma* spp.) by 940 µm, and in introduced European grasses by 800 µm. Differences in the absolute amount of EWT are evident between communities and are related to differences in the amount of live green biomass (Serrano et al. 2000). For example, ordering the plant communities by EWT, ceanothus and live oak are the highest, chamise is intermediate, and grasslands are the lowest, a finding that is consistent with the expected leaf area of these plants (Roberts et al. 1993, 1998).

Dry plant residues

Estimates of aboveground carbon storage, including woody stems and plant litter (i.e., senesced leaves and stems), could improve predictions of ecosystem processes (Asner et al. 1998, 1999). For example, increases in the dry litter fraction have been used in tropical forests and grasslands to estimate environmental stresses (Asner et al. 2003). The nutrient limitations of net primary productivity and carbon storage in humid tropical ecosystems have been estimated by combining LAI and dry residue indices (Asner et al. 1999). Carbon absorption features (see figure 1; nonphotosynthetic vegetation between 2000 and 2200 nm) are detectable in spectroscopic data. In sparse semiarid forests, the low canopy cover permits direct detection of plant litter, making it easier to estimate stand characteristics, disturbance condition, physiological state, and biogeochemical processes (Treuhaft et al. 2004). In semiarid shrublands and savannas, the abundance of potential fuel, in the form of dry plant litter and wood, can be used to assess wildfire risk (Asner et al. 1998, Roberts et al. 1998). The spatial patterns of dry plant residues in shrub and grassland ecosystems (figure 5) can be used to provide indicators of climate change and desertification (Ustin and Costick 1999, Asner and Green 2001).

Measures of structural carbon (cellulose, lignin, and other carbon compounds) provide a chlorophyll-independent estimate of biomass. Mapping concentrations of canopy lignin is a long-standing goal of biogeochemical research. However, the ability to obtain an independent measure of canopy lignin in spectroscopy data has been limited because of lignin's spectral similarity to cellulose and other cell wall materials. Using samples of ground dry leaves, Kokaly and Clark (1999)

found smaller errors in estimates of lignin than in estimates of cellulose, although cellulose comprised a substantially larger fraction of dry weight. Other researchers studying fresh and dry leaves have had difficulty retrieving separate lignin and cellulose concentrations (e.g., Fourty and Baret 1998) but better results for lumped estimates of dry plant matter.

Retrievals of dry plant residues require observations in the shortwave-infrared spectrum and are only measurable from high-fidelity, full-range imaging spectrometers (Roberts et al. 1993, Jacquemoud et al. 1996, Asner et al. 2003). Variations in LAI, chlorophyll, dry matter, and water content interact to cause nonlinear changes (Jacquemoud et al. 1995, Asner et al. 1998). Because changes in LAI have the greatest effect in the visible and near-infrared regions between 400 and 1300 nm, and dry plant residues have the greatest effect in the shortwave-infrared region between 2000 and 2400 nm (Asner 1998), observations of the full 400- to 2500-nm spectrum provide the best basis for quantitative estimates.

The quantity of dry plant material is a direct indicator of carbon production, turnover, and decomposition (heterotrophic respiration) (Turner et al. 2004). Asner and colleagues (2003) found that aboveground stocks of dry and live biomass were tightly coupled to soil organic carbon pools across a wide range of ecosystems in Argentina (figure 6). Because decomposition of surface litter is at least partially spatially and temporally correlated with soil decomposition and respiration, measures of non-green (i.e., nonphotosynthetic) plant material should help constrain soil carbon efflux. Recent studies (e.g., Högberg et al. 2001) demonstrate that recently fixed carbon, when available, contributes disproportionately to soil carbon efflux. Consequently, new studies are finding strong correlations between aboveground properties detectable with remote sensing (e.g., NDVI, water band) and ecosystem respiration (e.g., Boelman et al. 2003). These findings contradict the idea that respiration is inaccessible from remote sensing (e.g., Valentini et al. 2000).

Lidar, radar, and vegetation indices are relatively insensitive to ecosystems with the low biomass characteristic of semiarid systems (between 0 and 60 megagrams carbon per hectare [ha]), because of these systems' low leaf biomass and discontinuous canopies (Treuhaft et al. 2004, Wulder et al. 2004). Estimates of dry plant residues using the shortwave-infrared spectrum can help surmount these difficulties. Although arid and semiarid ecosystems (grassland, shrublands, savannas, and mesic woodlands) do not sequester large masses of carbon, and have low fluxes on a per-area basis, these ecosystems are the most abundant terrestrial landscapes, dominating about 40% of Earth's land surface, and are highly sensitive to climate perturbations.

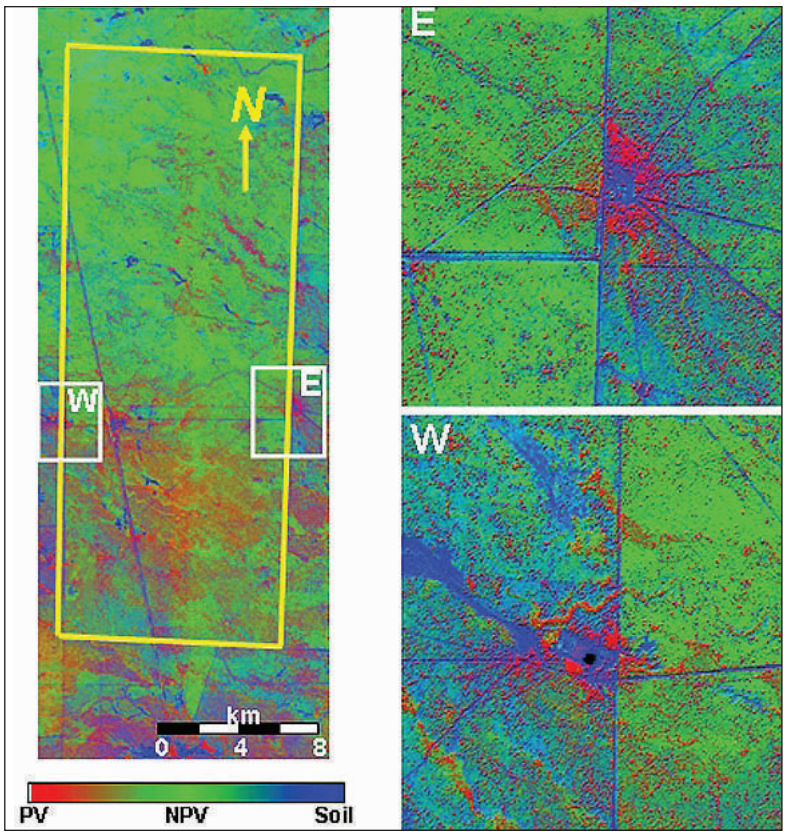

Figure 5. Spatial variation within the Nacunan Biosphere Reserve, Argentina, in three spectral end-members derived from AVIRIS (Airborne Visible/Infrared Imaging Spectrometer) data: 100% green vegetation (photosynthetic vegetation, or PV), 100% non-green vegetation (non-photosynthetic vegetation, or NPV), and 100% soil (displayed as red, green, and blue, respectively). Intermediate end-member mixtures are observed as shades between these colors. Modified from Asner and colleagues (2003).

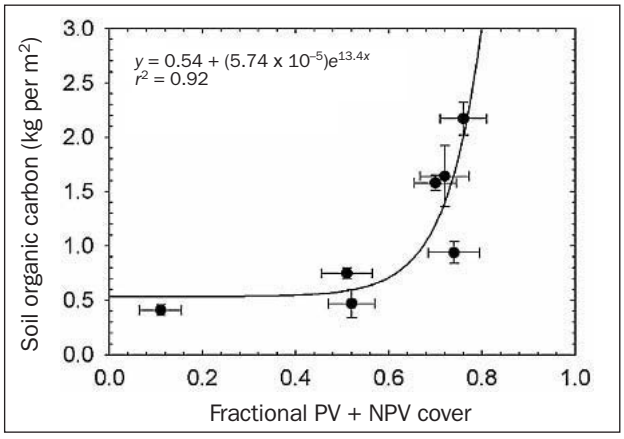

Figure 6. Fractional cover of green vegetation (photosynthetic vegetation, or PV) and dry residues (nonphotosynthetic vegetation, or NPV) measured by AVIRIS (Airborne Visible/Infrared Imaging Spectrometer) for a range of ecosystems in Argentina. Modified from Asner and colleagues (2003).

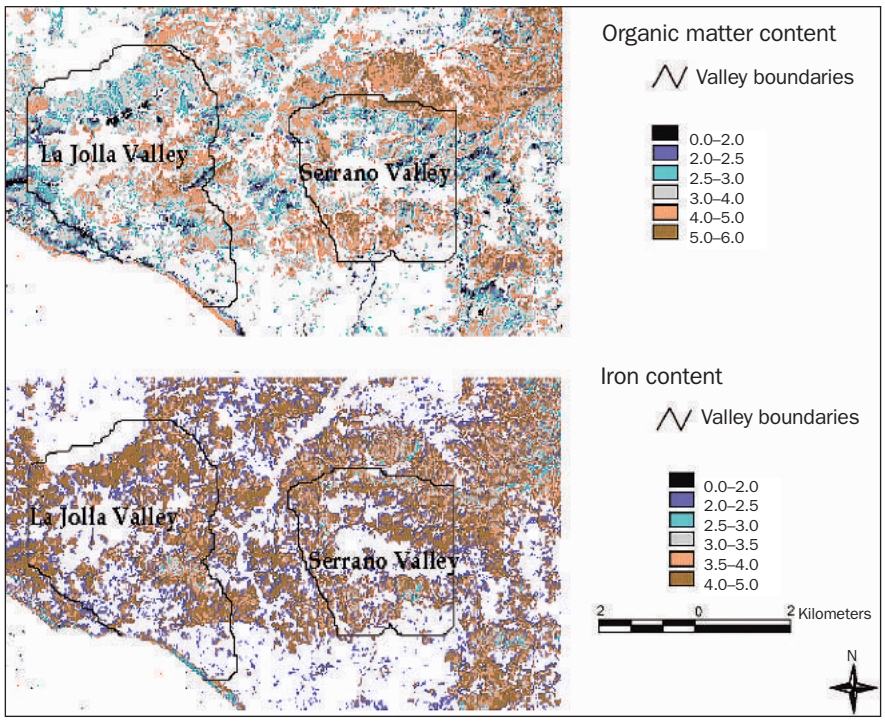

Figure 7. Hierarchical foreground and background analysis was used to quantify organic matter and iron oxide concentrations in two valleys in the Santa Monica Mountains, California. Data are from Palacios-Orueta and colleagues (1999).

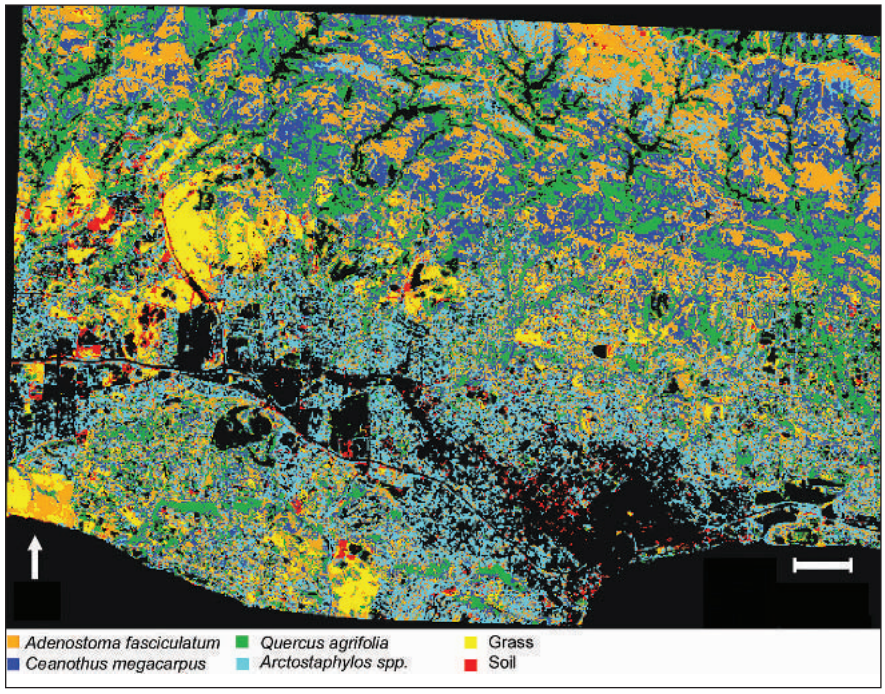

Figure 8. Vegetation map of the Santa Ynez Mountains, near Santa Barbara, California, using multiple end-member analysis of AVIRIS (Airborne Visible/Infrared Imaging Spectrometer) image data. Overall contingency matrix accuracy is estimated to be 89%. Modified from Dennison and Roberts (2003b).

Soil properties

Soils are highly variable, dynamic components of the environment, and sustainability of soil resources is essential for ecosystem function. Soils comprise a major repository for biospheric carbon, and organic matter in topsoil is a good indicator of soil quality, soil erosion, and physical processes such as hydraulic conductivity and soil aggregation. In the semiarid western United States, clays are associated with greater weathering, and expansive clays such as smectite increase erosion and mass wasting on poorly vegetated slopes. Calcium carbonate is also associated with erosion potential. Organic matter and clay mineralogy are correlated with soil characteristics such as cation exchange capacity, soil acidity, and the decomposition and sequestration of nitrogen, phosphorus, and sulfur.

It has long been recognized that some soil properties have spectral features that can be detected using spectroscopy (Ben-Dor et al. 1999). Baumgardner and colleagues (1985) identified five basic spectral shapes related to organic matter content, iron oxide content, and soil texture. Using factor analysis, Price (1990) and Huete and Escadafal (1991) found four basic combinations of soil properties. In general, soils, like plants, have only a few recognizable narrow absorption features. Soils typically have broad, shallow absorption features related to iron oxides and organic matter at wavelengths between 400 and 2500 nm. Reflectance decreases as organic matter increases. In soils with low levels of organic matter, the curve between 400 and 1000 nm is convex; in soils with high levels of organic matter, it is concave (Baumgardner et al. 1985). Ferric or ferrous iron causes absorptions in the visible and near-infrared spectra, particularly around 860 nm. In contrast to organic matter and iron oxides, various clay minerals (e.g., montmorillonite, kaolinite, illite, smectite) and carbonates have distinctive narrow-band absorptances in the shortwave-infrared region between 2000 and 2500 nm. Nonetheless, it is not simple to quantitatively estimate these soil properties. Soils are only accessible to airborne and satellite instruments in landscapes that have low vegetation cover. Typically, a

first step to detecting soil properties is to mask vegetated pixels. Palacios-Orueta and Ustin (1998), Palacios-Orueta and colleagues (1999), Hill and Schutt (2000), and Leone and Sommer (2000) have used vegetation masks, landform classes, and other hierarchical segregation methods to distinguish soil from vegetation.

Palacios-Orueta and Ustin (1998) showed that iron and organic matter content were the two main factors affecting spectral shape in soils from two valleys on the southern California coast. Palacios-Orueta and colleagues (1999) then used a hierarchical analysis to quantify soil organic matter and iron oxide concentrations from the same two valleys (figure 7), performing a two-step singular value decomposition that classified the soils first by their valley of origin and second by their concentrations of organic matter and iron oxides. The combined data were used to produce a map of the entire area. Despite complex topography and landscape heterogeneity, the results were within the range of measurement error obtained using standard wet chemical methods.

Mapping vegetation and land cover

Better discrimination of vegetation classes is obtained by measuring the many absorption features that narrow-band spectrometers can resolve. Because of its greater spectral dimensionality, spectroscopy discriminates among plant species more effectively than standard indices of vegetation and therefore has the potential to provide superior mapping capability. A number of studies have shown that community composition, and sometimes even species distribution, can be accurately mapped using imaging spectrometry. Zarco-Tejada and Miller (1999) exploited systematic species differences at the BOREAS (Boreal Ecosystem-Atmosphere Study) forest site by focusing on wavelengths that are sensitive to foliar chemistry. Fuentes and colleagues (2001) used both water content and the abundance of different plant pigments (figure 3) to produce extremely accurate local vegetation maps.

Figure 8 shows a vegetation map of a shrubland ecosystem located near Santa Barbara, California, created using multiple

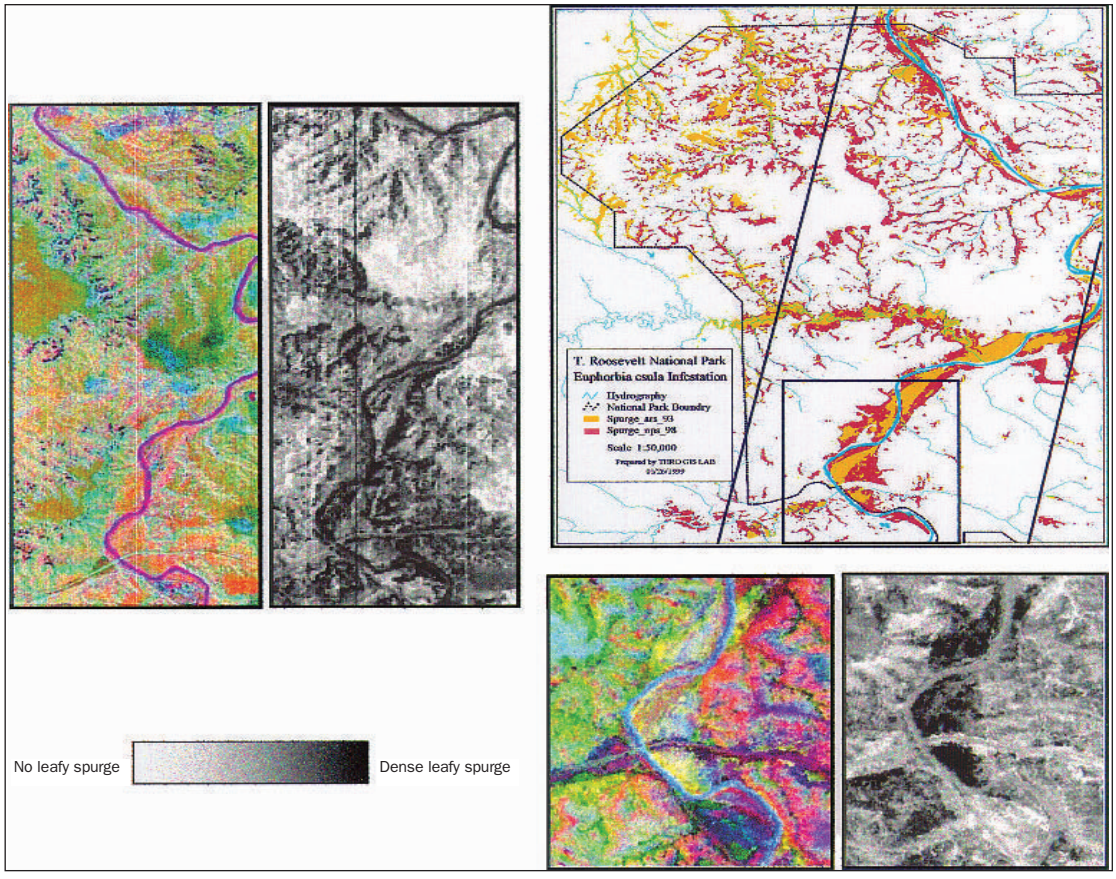

Figure 9. Leafy spurge in Theodore Roosevelt National Park, North Dakota. False-color minimum noise fraction (MNF) image (left) and grayscale spectral angle mapper (SAM) image (center) derived from Hyperion satellite data collected 6 July 2001. Upper right: National Park Service map of leafy spurge locations in 1993 (yellow) and 1998 (red), courtesy of Theodore Roosevelt National Park. The approximate location of the Hyperion flight line is shown on the map by the two diagonal bars. The box in the bottom center of that map depicts the location from which the AVIRIS (Airborne Visible/Infrared Imaging Spectrometer) data shown at lower right (false-color MNF image and grayscale SAM image) were collected on 21 June 2001. Source: Data courtesy of Ralph Root, US Geological Survey.

end-member analysis of AVIRIS data, in which the numbers and types of end-members were allowed to vary on a per-pixel basis (Roberts et al. 1998). Edaphic controls on the community distributions are evident. Chamise, manzanita, and ceanothus are distributed in parallel bands across the front range of the San Ynez Mountains; oak woodlands are concentrated in riparian sites and grasslands in flatter terrain.

Mapping and monitoring the spread of invasive species is recognized as the first step in eradicating these dangerous pests. Leafy spurge (*Euphorbia esula* L.) is an aggressive weed that causes severe ecosystem impacts throughout the northern United States. Theodore Roosevelt National Park, in North Dakota, has a major infestation; the weed grows throughout the park, especially west of the Little Missouri River and its tributaries. In 1970, only 13 ha (out of a total of 19,021) were infested with leafy spurge, but by 1993, 1700 ha were infested. Two spectral methods were used to identify the locations of the weeds within the matrix of the native vegetation. The first method used a form of principal components analysis (minimum noise fraction, or MNF) to reduce noise and compress the information into a few orthogonal transformed bands. The data were also analyzed using a spectral matching technique called the spectral angle mapper (SAM), an algorithm that classifies the similarity of pixels relative to a reference pixel (here, the mean spectrum of leafy spurge). With the aid of field-based training data, thresholds were identified that produced a best estimate for leafy spurge (see grayscale images in figure 9).

Figure 9 maps the distribution of leafy spurge in AVIRIS data (approximately 17-m pixels) and Hyperion data (approximately 30-m pixels) in the Little Missouri unit of Theodore Roosevelt National Park. The map on the upper right shows the distribution estimated from field studies and from composites of aerial photographs taken in 1993 and 1998. Leafy spurge increased its distribution along the Little Missouri River over this period. The riparian areas in the upper left of the field map, which showed leafy spurge infestation in 1993 but were not mapped in 1998, are areas where an integrated pest management program has controlled the spread of leafy spurge. The areas of leafy spurge infestation along the river in the field-based map are clearly identified in both the Hyperion and the AVIRIS images, although the color balance and the scaling of gray values vary somewhat between the two types of data. These examples illustrate the capability of imaging spectroscopy, operating from airborne or spaceborne platforms, to provide improved detail in maps of land cover.

Summary and future directions

Imaging spectroscopy is a cutting-edge technology, and its utility for ecological studies is virtually unlimited. A wide range of environmental applications have already been demonstrated, and analytical methods are becoming standardized. Data from imaging spectroscopy have repeatedly been shown to produce accurate estimates of many biochemical and physical characteristics related to key ecological processes. Spectroscopy is the only technology available to measure many important environmental properties over large regions, particularly canopy water content, dry plant residues, and soil biochemical properties.

Many potential users of imaging spectroscopy in the research community still believe that the instruments are either too experimental or too difficult for typical academic research laboratories to use. Significant advances in software for image processing and calibration, including availability of commercial packages, have greatly reduced the difficulty of analyzing and interpreting spectroscopy data for novice users. Advanced algorithms such as the MNF and SAM methods are available in easy-to-use commercial packages, as are a large number of additional routines. A number of commercial and governmental instruments are currently available on airplanes and space platforms, and more are planned; therefore, obtaining data for particular sites is less challenging than in the past. Web-based tools for teaching imaging spectroscopy are under development at the Virtual Center for Spatial Analysis and Remote Sensing (*http://vcsars.calstatela.edu*). Finally, NASA's AVIRIS data are public domain, and thousands of scenes are available from the NASA Jet Propulsion Laboratory archive (*http://aviris.jpl.nasa.gov*), an easy-to-view, Web-based archive that provides a basis for locating data of interest for new users.

Acknowledgments

We thank David Fuentes and Ralph Root for providing data and figures used in this article and Holly Manaker for assistance in preparing the figures for publication. We are also grateful to the National Aeronautics and Space Administration (NASA) Earth Science Enterprise for funding the research described in this article. A portion of this research was carried out at the Jet Propulsion Laboratory, California Institute of Technology, Pasadena, California, under contract with NASA.

References cited

Asner GP. 1998. Biophysical and biochemical sources of variability in canopy reflectance. Remote Sensing of Environment 64: 234–253.

Asner GP, Green RO. 2001. Imaging spectroscopy measures desertification in the Southwest U.S. and Argentina. Eos, Transactions of the American Geophysical Union 82: 601–606.

Asner GP, Wessman CA, Schimel DS, Archer S. 1998. Variability in leaf and litter optical properties: Implications for BRDF model inversions using AVHRR, MODIS, and MISR. Remote Sensing of Environment 63: 243–257.

Asner GP, Townsend AR, Bustamante MMC. 1999. Spectrometry of pasture condition and biogeochemistry in the Central Amazon. Geophysical Research Letters 26: 2769–2772.

Asner GP, Borghi C, Ojeda R. 2003. Desertification in Central Argentina: Regional changes in ecosystem carbon-nitrogen from imaging spectroscopy. Ecological Applications 13: 629–648.

Barton CVM, North PRJ. 2001. Remote sensing of canopy light use efficiency using the photochemical reflectance index: Model and sensitivity analysis. Remote Sensing of Environment 78: 264–273.

Baumgardner MF, Silva LF, Biehl LL, Stoner ER. 1985. Reflectance properties of soils. Advances in Agronomy 38: 1–44.

Ben-Dor E, Irons JR, Epema G. 1999. Soil reflectance. Pages 111–188 in Rencz AN, ed. Remote Sensing for the Earth Sciences. New York: John Wiley and Sons.

Boelman NT, Stieglitz M, Rueth HM, Sommerkorn M, Griffin KL, Shaver GR, Gamon JA. 2003. Response of NDVI, biomass, and ecosystem gas exchange to long-term warming and fertilization in wet sedge tundra. Oecologia 135: 414–421.

Carter GA. 1991. Primary and secondary effects of water content of the spectral reflectance of leaves. American Journal of Botany 78: 916–924.

Cohen WB, Goward SN. 2004. Landsat's role in ecological applications of remote sensing. BioScience 54: 535–545.

Curran PJ. 1989. Remote sensing of foliar chemistry. Remote Sensing of Environment 29: 271–278.

Davies A, Grant AMC. 1988. Near infrared spectroscopy for the analysis of specific molecules in food. Pages 46–51 in Creaser CS, Davies AMC, eds. Analytical Applications of Spectroscopy. London: Royal Society of Chemistry.

Dawson TP, Curran PJ, Plummer SE. 1998. LIBERTY—modeling the effects of leaf biochemical concentration on reflectance spectra. Remote Sensing of Environment 65: 50–60.

Dennison PE, Roberts DA. 2003a. The effects of vegetation phenology on endmember selection and species mapping in southern California chaparral. Remote Sensing of Environment 87: 295–309.

———. 2003b. Endmember selection for multiple endmember spectral mixture analysis using endmember average RMSE. Remote Sensing of Environment 87: 123–135.

Filella I, Peñuelas J. 1994. The red edge position and shape as indicators of plant chlorophyll content, biomass and hydric status. International Journal of Remote Sensing 15: 1459–1470.

Fourty T, Baret F. 1998. On spectral estimates of fresh leaf biochemistry. International Journal of Remote Sensing 19: 1283–1297.

Fuentes DA, Gamon JA, Qiu H-L, Sims DA, Roberts DA. 2001. Mapping Canadian boreal forest vegetation using pigment and water absorption features derived from the AVIRIS sensor. Journal of Geophysical Research 106: 33565–33577.

Gamon JA, Peñuelas J, Field CB. 1992. A narrow-waveband spectral index that tracks diurnal changes in photosynthetic efficiency. Remote Sensing of Environment 41: 35–44.

Ganapol BD, Johnson LF, Hammer PD, Hlavka CA, Peterson DL. 1998. LEAFMOD: A new within-leaf radiative transfer model. Remote Sensing of Environment 63: 182–193.

Gao B-C. 1996. NDWI—a normalized difference water index for remote sensing of vegetation liquid water from space. Remote Sensing of Environment 58: 257–266.

Gao B-C, Goetz AFH. 1995. Retrieval of equivalent water thickness and information related to biochemical components of vegetation canopies from AVIRIS data. Remote Sensing of Environment 52: 155–162.

Gitelson AA, Merzlyak MN. 1997. Remote estimation of chlorophyll content in higher plant leaves. International Journal of Remote Sensing 18: 2691–2697.

Hill J, Schutt B. 2000. Mapping complex patterns of erosion and stability in dry Mediterranean ecosystems. Remote Sensing of Environment 74: 557–569.

Högberg P, Nordgren A, Buchmann N, Taylor AFS, Ekblad A, Högberg MN, Nyberg G, Ottosson-Löfvenius M, Read DJ. 2001. Large-scale forest girdling shows that current photosynthesis drives soil respiration. Nature 411: 789–792.

Huete AR, Escadafal R. 1991. Assessment of biophysical soil properties through spectral decomposition techniques. Remote Sensing of Environment 35: 149–159.

Jacquemoud S, Baret F, Andrieu B, Danson FM, Jaggard K. 1995. Extraction of vegetation biophysical parameters by inversion of the PROSPECT + SAIL models on sugar beet canopy reflectance data. Application to TM and AVIRIS sensors. Remote Sensing of Environment 52: 163–172.

Jacquemoud S, Ustin SL, Verdebout J, Schmuck G, Andreoli G, Hosgood B. 1996. Estimating leaf biochemistry using the PROSPECT leaf optical properties model. Remote Sensing of Environment 56: 194–202.

Kokaly RF. 2001. Investigating a physical basis for spectroscopic estimates of leaf nitrogen concentration. Remote Sensing of Environment 75: 153–161.

Kokaly RF, Clark RN. 1999. Spectroscopic determination of leaf biochemistry using band-depth analysis of absorption features and stepwise multiple linear regression. Remote Sensing of Environment 67: 267–287.

Leone AP, Sommer S. 2000. Multivariate analysis of laboratory spectra for the assessment of soil development and soil degradation in the southern Apennines (Italy). Remote Sensing of Environment 72: 346–359.

Lichtenthaler HK, Gitelson A, Lang M. 1996. Non-destructive determination of chlorophyll content of leaves of a green and an aurea mutant of tobacco by reflectance measurements. Journal of Plant Physiology 148: 483–493.

Martin ME, Aber JD. 1997. High spectral resolution remote sensing of forest canopy lignin, nitrogen, and ecosystem processes. Ecological Applications 7: 431–443.

Palacios-Orueta A, Ustin SL. 1998. Remote sensing of soils in the Santa Monica Mountains, pt. I: Spectral analysis. Remote Sensing of Environment 65: 170–1183.

Palacios-Orueta A, Pinzón J, Ustin SL, Roberts DA. 1999. Remote sensing of soils in the Santa Monica Mountains, pt. II: Hierarchical foreground and background analysis. Remote Sensing of Environment 68: 138–151.

Peñuelas J, Piñol J, Ogaya R, Filella I. 1997. Estimation of plant water concentration by the reflectance Water Index WI (R900/R970). International Journal of Remote Sensing 18: 2869–2875.

Price JC. 1990. On the information content of soil reflectance spectra. Remote Sensing of Environment 33: 113–121.

Rahman AF, Gamon JA, Fuentes DA, Roberts DA, Prentiss D. 2001. Modeling spatially distributed ecosystem flux of boreal forests using hyperspectral indices from AVIRIS imagery. Journal of Geophysical Research 106: 33579–33591.

Roberts DA, Smith MO, Adams JB. 1993. Green vegetation, nonphotosynthetic vegetation, and soils in AVIRIS data. Remote Sensing of Environment 44: 255–269.

Roberts DA, Gardner M, Church R, Ustin S, Scheer G, Green RO. 1998. Mapping chaparral in the Santa Monica Mountains using multiple endmember spectral mixture models. Remote Sensing of Environment 65: 267–279.

Rock BN, Hoshizaki T, Miller JR. 1988. Comparison of *in situ* and airborne spectral measurements of the blue shift associated with forest decline. Remote Sensing of Environment 24: 109–127.

Running SW, Nemani RR, Heinsch FA, Zhao M, Reeves M, Hashimoto H. 2004. A continuous satellite-derived measure of global terrestrial primary production. BioScience 54: 547–560.

Sanderson EW, Zhang M, Ustin SL, Rejmankova E. 1998. Geostatistical scaling of canopy water content in a California salt marsh. Landscape Ecology 13: 79–92.

Serrano L, Ustin SL, Roberts DA, Gamon JA, Peñuelas J. 2000. Deriving water content of chaparral vegetation from AVIRIS data. Remote Sensing of Environment 74: 570–581.

Treuhaft RN, Law BE, Asner GP. 2004. Forest attributes from radar interferometric structure and its fusion with optical remote sensing. BioScience 54: 561–571.

Turner DP, Ollinger SV, Kimball JS. 2004. Integrating remote sensing and ecosystem process models for landscape- to regional-scale analysis of the carbon cycle. BioScience 54: 573–584.

Ustin SL, Costick LA. 1999. Multispectral remote sensing over semi-arid landscapes for resource management. Pages 97–112 in Hill MJ, Aspinall RJ, eds. Spatial Information for Land Management. Reading (United Kingdom): Gordon and Breach.

Ustin SL, Roberts DA, Jacquemoud S, Pinzón J, Gardner M, Scheer GJ, Castaneda CM, Palacios A. 1998. Estimating canopy water content of chaparral shrubs using optical methods. Remote Sensing of Environment 65: 280–291.

Valentini R, et al. 2000. Respiration as the main determinant of carbon balance in European forests. Nature 404: 861–864.

Weiss M, Baret F. 1999. Evaluation of canopy biophysical variable retrieval performances from the accumulation of large swath satellite data. Remote Sensing of Environment 70: 293–306.

Wessman CA. 1990. Evaluation of canopy biochemistry. Pages 135–156 in Hobbs RJ, Mooney HA, eds. Remote Sensing of Biosphere Functioning. New York: Springer-Verlag.

Wulder M. 1998. Optical remote-sensing techniques for the assessment of forest inventory and biophysical parameters. Progress in Physical Geography 22: 449–476.

Wulder MA, Hall RJ, Coops NC, Franklin SE. 2004. High spatial resolution remotely sensed data for ecosystem characterization. BioScience 54: 511–521.

Zarco-Tejada PJ, Miller JR. 1999. Land cover mapping at BOREAS using red edge spectral parameters from CASI imagery. Journal of Geophysical Research–Atmospheres 104: 27921–27933.

Zarco-Tejada PJ, Ustin SL. 2001. Modeling canopy water content for carbon estimates from MODIS data at land EOS validation sites. Pages 342–344 in IGARSS 2001: Scanning the Present and Resolving the Future. Proceedings, IEEE 2001 International Geoscience and Remote Sensing Symposium, 9–13 July 2001, University of New South Wales, Sydney, Australia. New York: IEEE.

Zhang M, Ustin SL, Rejmankova E, Sanderson EW. 1996. Remote sensing of salt marshes: Potential for monitoring. Ecological Applications 7: 1039–1053.